

# Two-level design for aperiodic networked control systems<sup>☆</sup>



Azhar M. Memon<sup>a</sup>, Magdi S. Mahmoud<sup>b,\*</sup>

<sup>a</sup> Center for Engineering Research, Research Institute (CER-RI), King Fahd University of Petroleum and Minerals, Dhahran 31261, Saudi Arabia

<sup>b</sup> Systems Engineering Department, King Fahd University of Petroleum and Minerals, Dhahran 31261, Saudi Arabia

## ARTICLE INFO

### Article history:

Received 1 April 2015

Received in revised form

26 July 2015

Accepted 26 August 2015

Available online 6 September 2015

### Keywords:

$\mathcal{H}_\infty$  controller

Modified IEEE 802.15.4 protocol

Networked control

Priority-based scheduling (PBS)

Self-triggering

Two-level design

## ABSTRACT

Two critical issues in networked control systems are coupling of control and communication, and energy economy, especially for battery powered wireless sensor nodes. In this regard, a two-level design procedure for multiple loops with  $\mathcal{H}_\infty$  based self-triggered control applied over the modified IEEE 802.15.4 wireless protocol is presented. Control and communication are decoupled by introducing an upper-bound on the transmission rate, and optimal usage of communication bandwidth and energy is guaranteed by modifying the wireless protocol. The presented priority-based scheduling algorithm can accommodate more systems as compared with the number of available transmission slots, while being efficient in terms of computational load and energy consumption. Simulation results show a significant reduction in energy expenditure in terms of decrease in duty cycle as compared with the periodic implementation.

© 2015 Elsevier B.V. All rights reserved.

## 1. Introduction

With an increasing trend of wireless networked feedback loops using aperiodic triggering mechanisms, the demand to decouple control and communication designs [1], and to optimize computational cost, communication load, and energy consumption has also increased [2]. The standard implementations of feedback control over a network or embedded platform use periodic scheme; although this approach decouples communication from control and a mature systems theory exists which eases the implementation, it causes an enormous waste of energy and communication capabilities, particularly when there is no need for a corrective feedback signal. In contrast, the aperiodic implementations (event- and self-triggered (ET and ST)), while saving considerable amount

of energy and communication resources [3], introduce correlation between the states of participating control loops in networked control system (NCS), which complicates the interaction between control and communication.

Both ET and ST schemes comprise two elements, a controller and a triggering mechanism. For ET, the triggering takes place on the sensor side, while in ST, the triggering time is *predicted by the controller*. Specifically, in former, the sensor node determines on the basis of a comparison between the present state and a threshold, if the information to the controller should be sent. For ST, the controller initiates the triggering at the predicted sampling time for the sensor node to transmit the state.

As compared with the periodic setting, this significantly reduces the amount of required communication, however for ET, the computational cost at the sensing node increases due to continuous monitoring of the plant state which is not well-suited for the battery powered sensor nodes. Furthermore, it might require a dedicated hardware to check the event condition. ST mechanism was introduced in [4] as a remedy to this problem. This scheme does not require continuous checking of the state as the

<sup>☆</sup> This work is supported by the deanship for scientific research at KFUPM through research group project **RG-1316-1**.

\* Corresponding author.

E-mail addresses: [azharmehmood@kfupm.edu.sa](mailto:azharmehmood@kfupm.edu.sa) (A.M. Memon), [msmahmoud@kfupm.edu.sa](mailto:msmahmoud@kfupm.edu.sa) (M.S. Mahmoud).

controller predicts update-time on the basis of previously sampled state and plant dynamics. Hence, ET mechanism is reactive and ST is proactive.

Some recent results on the subject of NCSs with time-delays and packet dropouts are reported in [5–8]. Specifically, [5] presented the model of multi-rate NCSs with a novel approach combining linear switched control systems with communication sequence. Additionally, the authors proposed the conditions of controllability and observability. The problem of distributed fuzzy filter design for sensor networks described by discrete-time T–S fuzzy systems was addressed in [6]. Distributed fuzzy filters guaranteed the filtering error dynamic system to be mean-square asymptotically stable with an average  $\mathcal{H}_\infty$  performance. Another work regarding  $\mathcal{H}_\infty$  filtering problem was presented in [7] for discrete-time networked nonlinear systems. A predictive control scheme was employed in [8] to compensate for the network-induced time-delays in NCS. However, all these works employed periodic transmission of information over the network.

In the context of ET to decouple communication from control, [1] limited the usage of communication channel in terms of maximum allowable transmission rate, which depended upon the maximum number of transmission slots offered by the channel. The authors used the solution of stochastic optimal control problem in order to determine optimal transmission rate for each system. However, ET mechanism was used without the provision for energy saving. In the context of ET filtering,  $\mathcal{H}_\infty$ -based filtering problem was considered in [9] for a network with communication delays. Additionally, ET fuzzy filtering for a class of nonlinear systems was considered in [10] recently.

As an attractive aperiodic scheme, ST methodology has been studied in many works with prominent studies being [11] and [12] which presented the solution of ST based  $\mathcal{H}_2$  and  $\mathcal{H}_\infty$  optimal control problems, [13] and [14] which showed finite-gain  $\mathcal{L}_2$  stability of linear systems effected by bounded disturbances, [15] for ST based model predictive control, and [16] for the development of ST based LQR controller.

IEEE 802.15.4 wireless protocol, which forms the basis for industrial standards like WirelessHART and ISA100, has been the center of attention since its availability as the low data-rate and energy-efficient protocol [17–19]. Some of the highlighted works that fall in the domain of network modeling, optimization, and stability analysis of the network for control of multiple loops sharing common wireless network to close the feedback loops can be found in [20–23].

Works which study ST control over IEEE 802.15.4 network are: [24], which considered energy consumption issues in the network by adapting the MAC layer parameters for single control loop setting, [25] considered a model-based ST strategy to control single control loop over an adaptive IEEE 802.15.4 network, [19] also tailored the protocol parameters to enhance energy savings at the expense of increased computational cost because the methodology used a disturbance estimator and two-step ahead triggering time predictor. [26] focused on ET, ST, and hybrid techniques to minimize energy consumption in sensor/actuator networks without taking IEEE 802.15.4

protocol into consideration, [27] and [28] implemented modified MAC layer of IEEE 802.15.4 protocol in order to suit the particular requirements of ST control and compared it against periodic scheme to demonstrate a significant reduction in energy consumption. [29] also altered the protocol for flexible implementation of ET, ST, and hybrid communication mechanisms. The experimental results showed significant reduction in energy consumption as compared with the periodic implementation.

### 1.1. Contributions

In view of the studies mentioned above and existing results, to the best of authors' knowledge, the present literature lacks in:

- Taking advantage of the proactive nature of ST methodology which provides the triggering time *in advance*.
- The provision of including more control loops than the maximum number of transmission slots.
- A decoupled design of communication and control in multiple control loop setting, which saves computational resources besides energy efficiency.

These form the main motivation for this work which has the following contributions and significance:

(a) Two-level design method for NCS in which control and communication designs are decoupled. The first level is based on ST  $\mathcal{H}_\infty$  controller and the second level comprises the network manager (NM).

(b) Modifications in IEEE 802.15.4 protocol to benefit from ST control. Specifically, the predicted triggering time is used to schedule the next beacon interval thus saving considerable amount of energy at the sensor node, which enhances energy efficiency of the applications based on IEEE 802.15.4 protocol. Additionally, this characteristic can avoid contention and congestion in the network.

(c) Priority based scheduling (PBS) algorithm is integrated in the modified protocol to accommodate more systems than the maximum number of available transmission slots.

(d) The proposed design does not require two-steps ahead triggering time predictor and a disturbance observer, as opposed to [19], thus saving computational cost.

**Organization:** The paper is organized as follows: [Section 2](#) defines the problem and gives an overview of the design. [Sections 3](#) and [4](#) present first and second level controllers, respectively. Simulation results are given in [Section 5](#), and [Section 6](#) concludes the paper. The proofs of forthcoming lemmas and theorems are given in appendix.

**Notations:** Sets of real numbers and integers are denoted by  $\mathbb{R}$  and  $\mathbb{Z}$ , respectively. Set of strictly positive real numbers are represented by  $\mathbb{R}^+$  and those including zero are denoted as  $\mathbb{R}^{[0,+]}$ . The set of positive definite and semi-definite integers are represented as  $\mathbb{Z}^+$  and  $\mathbb{Z}^{[0,+]}$ , respectively. The second norm is given as  $\|\cdot\|_2$ .

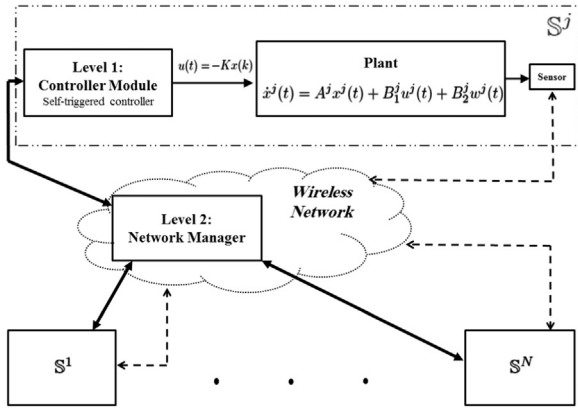


Fig. 1. NCS with two-level control. Solid lines: wired connection; dashed lines: wireless link.

## 2. Problem definition and overview

A class of  $N$  independent  $\mathcal{H}_\infty$  based ST control systems is considered. The feedback loops of these systems are closed over the same wireless communication medium as shown in Fig. 1. The controllers are wired with the NM, and sensor nodes acquire all the states and transmit to the NM wirelessly. This type of setting, which follows star topology for sensor-controller network and wired connections for controller-actuator link, is common in industrial applications such as process control [19]. Each system  $\mathcal{S}^j$ , where  $j \in \{1, \dots, N\}$ , implements a ST  $\mathcal{H}_\infty$  controller to ensure finite-gain  $\mathcal{L}_2$  stability. In particular, the results of [14] are extended to incorporate the constraints introduced on triggering time, as explained in Section 3. The wireless network uses a slotted communication mechanism which is based on the modifications proposed to IEEE 802.15.4 protocol. The controllers requesting state information are assigned fixed time slots according to their predicted triggering times. NM gets state information from sensor nodes in their respective time slots, and passes this information to respective controllers.

Due to limited bandwidth of the communication network, the number of time slots is restricted to  $N_{max}$  in each beacon interval [17]. The aim is to guarantee finite-gain  $\mathcal{L}_2$  stability using  $\mathcal{H}_\infty$  controllers for all the control loops, while reducing the communication cost. However, due to correlation introduced between the states of the systems because of a bandwidth-limited communication medium, this problem is difficult to solve. In order to decouple communication from control and avoid Zeno behavior, the transmission interval of each system is lower-bounded by minimum inter-sampling period (or maximum transmission rate)  $\tau \in \mathbb{R}^+$ . This splits the problem into two levels.

At the first level, ST controller module for each system guarantees  $\mathcal{L}_2$  stability using full-information  $\mathcal{H}_\infty$  controller, besides computing next sampling time. These controllers send their *System's Overall State Indicator (SOSI)* and *next sampling times* to the second level controller through the wired connection, as soon as they finish the computations. At the second level the NM, which is based on the proposed modifications in IEEE 802.15.4 protocol, implements PBS algorithm which uses this information of

each plant to schedule their transmissions. Moreover, unlike [19] the proposed PBS mechanism does not require a disturbance observer and two-steps ahead triggering-time predictor, which imply less computational load.

Here two cases are considered: first, when the number of control loops is at-most  $N_{max}$ , and second, when this number exceeds  $N_{max}$ . For this work,  $N \leq N_{max} + 1$  is considered as the bound on the number of systems for second case. In first case, all the systems are allowed to transmit, i.e., no transmission request is denied while optimizing the bandwidth usage. In second scenario, PBS accepts transmission requests of only those systems which encounter more performance degradation (revealed by SOSI) as compared with the other system, for which the transmission slot is postponed. In this way, the proposed methodology can accommodate more systems than the number of available transmission slots, as opposed to [19].

## 3. First level: ST $\mathcal{H}_\infty$ controller

The  $j$ th control system  $\mathcal{S}^j$ , where  $j \in \{1, \dots, N\}$ , consists of a plant  $\mathcal{P}^j$ , a controller module  $\mathcal{C}^j$ , and a sensor  $\mathcal{S}^j$ . The plants have continuous-time linear dynamics described as [14]

$$\begin{aligned} \dot{x}^j(t) &= A^j x^j(t) + B_1^j u^j(t) + B_2^j w^j(t), \\ u^j(t) &= -B_1^{j,T} P^j x^j(t) = -K^j x^j(t), \end{aligned} \quad (1)$$

where  $x^j(t) \in \mathbb{R}^n$  is  $j$ th system's state vector,  $u^j(t) \in \mathbb{R}^m$  is the control input,  $w^j(t) \in \mathbb{R}^l$  is the exogenous disturbance in  $\mathcal{L}_2$  space, and the matrices  $A^j \in \mathbb{R}^{(n \times n)}$ ,  $B_1^j \in \mathbb{R}^{(n \times m)}$  and  $B_2^j \in \mathbb{R}^{(n \times l)}$  represent the system model.

The positive-definite symmetric matrix  $P^j$  represents the solution of the following  $\mathcal{H}_\infty$  ARE:

$$P^j A^j + A^{j,T} P^j - P^j B_1^j B_1^{j,T} P^j + I + \frac{1}{\gamma^{j,2}} P^j B_2^j B_2^{j,T} P^j = 0, \quad (2)$$

for some  $\gamma^j > 0$ . For the ease of notation, superscript  $j$  is dropped in the forthcoming analysis.

The controller module is a digital system which performs two sets of tasks. In the first set, it receives the sampled state and computes the control input. In the second set, it computes the next sampling time and SOSI, and sends this information to the NM. The timing diagram in Fig. 2 illustrates these steps.

Let  $k \in \mathbb{Z}^{(0,+)}$ , then at time instants  $\delta_k \in \mathbb{R}^{(0,+)}$  the controller performs first set of computations which takes  $\Delta_{k,1} \in \mathbb{R}^+$  units of time. As soon as the controller module completes these calculations, it applies the control input on the plant at  $\rho_k \in \mathbb{R}^{(0,+)}$  and also starts the second set of computations; in this way, the time taken for the second set does not affect the control function. For  $\Phi_k \in \mathbb{R}^+$  units of time, this control input is held constant until the next finishing time  $\rho_{k+1}$ . This renders (1) as a sampled-data system,

$$\begin{aligned} \dot{x}(t) &= Ax(t) + B_1 u(t) + B_2 w(t), \\ u(t) &= -B_1^T P x(k) = -Kx(k), \quad \forall t \in (\rho_k, \rho_{k+1}), \end{aligned} \quad (3)$$

where  $x(k)$  denotes the state sampled at  $\delta_k$ .

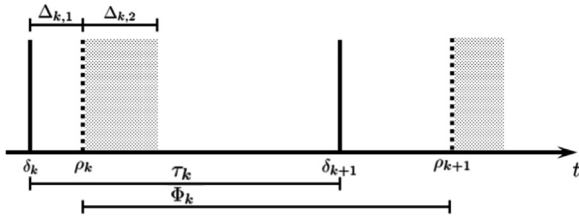


**Fig. 2.** Timing diagram. Controller module performs two sets of computations; first set:  $\Delta_{k,1}$ , second set:  $\Delta_{k,2}$ .

**Definition 3.1** (Wang and Lemmon [14]). Sampled-data system (3) is said to be finite-gain  $\mathcal{L}_2$  stable from  $w$  to  $x$  with an induced gain less than  $\gamma > 0$ , if there exists non-negative constant  $\epsilon$  such that

$$\left( \int_0^\infty \|x(t)\|_2^2 dt \right)^{1/2} \leq \gamma \left( \int_0^\infty \|w(t)\|_2^2 dt \right)^{1/2} + \epsilon, \quad (4)$$

for any  $w$  satisfying  $(\int_0^\infty \|w(t)\|_2^2 dt)^{1/2} < \infty$ .

The aperiodic inter-sampling time, denoted by  $\tau_k$ , is both upper and lower-bounded as

$$\underline{\tau} \leq \tau_k = \delta_{k+1} - \delta_k \leq \bar{\tau}, \quad \forall k \in \mathbb{Z}^+, \quad (5)$$

where  $\bar{\tau} \in \mathbb{R}^+$  represents the upper-bound to ensure bounded latency, and  $\underline{\tau}$  is the lower-bound to decouple control and communication. The choice of these bounds is made according to the dynamics of the participating systems in the NCS, while satisfying the communication constraints imposed by the protocol. Before the ST  $\mathcal{H}_\infty$  scheme is presented which ensures finite-gain  $\mathcal{L}_2$  stability, the following assumption is stated.

**Assumption 1.** The computational delays  $\Delta_{k,1}$  and  $\Delta_{k,2}$  (Fig. 2) are negligible as compared with the inter-sampling time  $\tau_k$ . This assumption is realistic because firstly, the low data-rate wireless network is suitable for low-speed control applications which do not require very fast sampling. Secondly, the controller module and NM have high-speed computational power. Both these facts imply that  $\Delta_{k,1} + \Delta_{k,2} \ll \tau_k$ , hence  $\delta_k = \rho_k$  for all  $k \in \mathbb{Z}^+$ .

**Lemma 1** (Wang and Lemmon [14]). For  $j$ -th sampled-data system given as (3) with Assumption 1, let  $V: \mathbb{R}^n \rightarrow \mathbb{R}^+$  be a positive semi-definite function defined by  $V(x) = x^T P x$  with  $P$  given in (2). For any real constant  $\beta \in (0, 1]$ , the directional derivative of  $V$  satisfies

$$\dot{V} \leq -\beta^2 \|x(t)\|_2^2 + \gamma^2 \|w(t)\|_2^2 + (e_t^k)^T M e_t^k - x^T(k) N x(k), \quad \forall t \in [\delta_k, \delta_{k+1}), \quad (6)$$

for all  $k \in \mathbb{Z}^+$ , where  $e_t^k = x(t) - x(k)$  represents the measurement error. The matrices  $M$  and  $N$  are defined as

$$M = (1 - \beta^2)I + P B_1 B_1^T P; \quad N = \frac{1}{2}(1 - \beta^2)I + P B_1 B_1^T P. \quad (7)$$

The proof of this lemma is given in [14] and left for brevity.

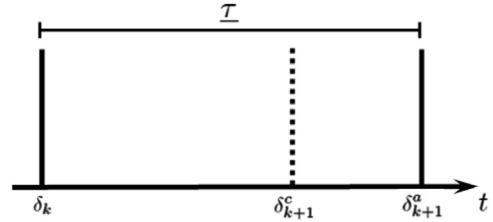


**Fig. 3.** When the computed triggering time  $\delta_{k+1}^c < \underline{\tau}$  then the system is assigned  $\delta_{k+1}^a$  such that  $\delta_{k+1}^a - \delta_k = \underline{\tau}$ .

From (6), finite-gain  $\mathcal{L}_2$  stability is guaranteed as long as the following inequality is satisfied:

$$(e_t^k)^T M e_t^k \leq x^T(k) N x(k), \quad \forall t \in [\delta_k, \delta_{k+1}). \quad (8)$$

Since it is assumed that the disturbance can be any signal in  $\mathcal{L}_2$  space, it is necessary to show that the error  $\|\sqrt{M}e_t^k\|_2$  remains bounded for all  $t \in [\delta_k, \delta_{k+1})$ . Furthermore, there can be a case wherein the NM assigns  $\delta_{k+1}^a$  to a control loop if it demands to sample the state at  $\delta_{k+1}^c$  such that  $\delta_{k+1}^c < \delta_{k+1}^a$ , where the superscripts  $c$  and  $a$  denote the computed and assigned triggering times, respectively. This covers both the cases, i.e., (1) when the demanded time falls below  $\underline{\tau}$  i.e., if  $\delta_{k+1}^c - \delta_k < \underline{\tau}$ , as shown in Fig. 3, and (2) when the NM assigns a different time slot when implementing PBS algorithm. These facts necessitate to show that the error remains bounded during the interval  $t \in [\delta_{k+1}^c, \delta_{k+1}^a)$ .

Following lemma shows that these bounds indeed exist. For the ease of analysis, following notations are defined:

$$\begin{aligned} \mu(x) &= \|\sqrt{N}x\|_2; \quad \mu_0(x(k)) = \|\sqrt{M}A x(k)\|_2; \\ \alpha &= \|\sqrt{M}A\sqrt{M}^{-1}\|_2, \end{aligned} \quad (9)$$

where  $\bar{A} = A - B_1 B_1^T P$  represents the closed-loop matrix. Here it is assumed that

**Assumption 2.** For a bounded constant  $\tau' > 0$ ,

$$0 < \delta_{k+1}^a - \delta_{k+1}^c \leq \tau',$$

i.e., the difference between computed and assigned triggering times is uniformly bounded.

**Lemma 2 (Case 1:  $\delta_{k+1}^a = \delta_{k+1}^c$ ).** For the sampled-data system (3) with Assumption 1, let  $\beta \in (0, 1]$  be such that the matrix  $M$  defined in (7) has full rank. The following inequality must hold for all  $t \in [\delta_k, \delta_{k+1})$ :

$$\begin{aligned} \|\sqrt{M}e_t^k\|_2 &\leq \frac{\mu_0(x(k))}{\alpha} (e^{\alpha(t-\delta_k)} - 1) \\ &\quad + \int_{\delta_k}^t e^{\alpha(t-s)} \|\sqrt{M}B_2\|_2 \|w(s)\|_2 ds. \end{aligned} \quad (10)$$

**Case 2:  $\delta_{k+1}^a > \delta_{k+1}^c$ .**

For the sampled-data system (3) with Assumptions 1 and 2, let  $\beta \in (0, 1]$  be such that the matrix  $M$  defined in (7) has full rank. The following inequality must hold for all  $t \in [\delta_{k+1}^c, \delta_{k+1}^a)$ :

$$\|\sqrt{M}e_t^k\|_2 \leq \frac{\mu_0(x(k))}{\alpha} (e^{\alpha(t-\delta_k)} - 1)$$

$$\begin{aligned}
& + \int_{\delta_{k+1}^c}^t e^{\alpha(t-s)} \|\sqrt{MB_2}\|_2 \|w(s)\|_2 ds \\
& + e^{\alpha(t-\delta_{k+1}^c)} \int_{\delta_k}^{\delta_{k+1}^c} e^{\alpha(\delta_{k+1}^c-s)} \|\sqrt{MB_2}\|_2 \|w(s)\|_2 ds.
\end{aligned} \quad (11)$$

With the error bounds given in Lemma 2, (10) and (11) are substituted in (6) to obtain an upper-bound on  $\dot{V}$  in terms of the induced gain. It is natural to expect that the gain will be upper- and lower-bounded due to the bounds defined in (5) for the first case, and for the second case, an additional term will be added due to the difference between computed and assigned triggering times.

**Theorem 3 (Case 1:  $\delta_{k+1}^a = \delta_{k+1}^c$ ).** Consider the sampled-data system (3) with Assumption 1. Let

- $\beta \in (0, 1]$  be such that the matrix  $M$  defined in (7) has full rank, and
- the bounded constants  $\bar{\tau}$ ,  $\underline{\tau}$ ,  $\underline{\Gamma}$ ,  $\bar{\Gamma} \in \mathbb{R}^+$ .

If for any  $k \in \mathbb{Z}^+$ , the inequalities

$$\delta_k < \delta_{k+1}, \quad (12)$$

$$\underline{\tau} \leq \tau_k \leq \bar{\tau}, \quad (13)$$

$$\zeta(x(k), \delta_k, \delta_{k+1}) \leq \int_{\delta_k}^{\delta_{k+1}} x^T(k) N x(k) dt, \quad (14)$$

hold where

$$\begin{aligned}
\zeta(x(k), \delta_k, \delta_{k+1}) \\
= \frac{2\mu_0^2}{\alpha^3} \left[ 2\alpha(\delta_{k+1} - \delta_k) - 4e^{\alpha(\delta_{k+1} - \delta_k)} + e^{2\alpha(\delta_{k+1} - \delta_k)} + 3 \right],
\end{aligned} \quad (15)$$

then the sampled-data system (3) is said to be finite-gain  $\mathcal{L}_2$  stable from  $w$  to  $x$  with an induced gain bounded between  $\underline{\Gamma}$  and  $\bar{\Gamma}$ , where

$$\begin{aligned}
\underline{\Gamma} &= \frac{1}{\alpha} \left[ \alpha^2 \gamma^2 + 4 \|\sqrt{MB_2}\|_2^2 (e^{\alpha \underline{\tau}} - 1)^2 \right]^{1/2}; \\
\bar{\Gamma} &= \frac{1}{\alpha} \left[ \alpha^2 \gamma^2 + 4 \|\sqrt{MB_2}\|_2^2 (e^{\alpha \bar{\tau}} - 1)^2 \right]^{1/2}.
\end{aligned} \quad (16)$$

**Case 2:  $\delta_{k+1}^a > \delta_{k+1}^c$**

Consider the sampled-data system (3) with Assumptions 1 and 2. Let

- $\beta \in (0, 1]$  be such that the matrix  $M$  defined in (7) has full rank, and
- the bounded constants  $\xi_k$ ,  $\bar{\tau}$ ,  $\underline{\tau}$ ,  $\underline{\Gamma}$ ,  $\bar{\Gamma} \in \mathbb{R}^+$ .

If for any  $k \in \mathbb{Z}^+$ , the inequalities

$$\delta_k < \delta_{k+1}, \quad (17)$$

$$\underline{\tau} \leq \tau_k \leq \bar{\tau}, \quad (18)$$

$$\eta(x(k), \delta_{k+1}^c, \delta_{k+1}^a) \leq \int_{\delta_{k+1}^c}^{\delta_{k+1}^a} x^T(k) N x(k) dt + \xi_k (\delta_{k+1}^a - \delta_{k+1}^c), \quad (19)$$

hold where

$$\begin{aligned}
\eta(x(k), \delta_{k+1}^c, \delta_{k+1}^a) \\
= \frac{2\mu_0^2}{\alpha^3} \left[ 2\alpha(\delta_{k+1}^a - \delta_{k+1}^c) + e^{-2\alpha\delta_k} (e^{\alpha\delta_{k+1}^a} - e^{\alpha\delta_{k+1}^c}) \right. \\
\left. \times (e^{\alpha\delta_{k+1}^a} + e^{\alpha\delta_{k+1}^c} - 4e^{\alpha\delta_k}) \right],
\end{aligned} \quad (20)$$

then the sampled-data system (3) is said to be finite-gain  $\mathcal{L}_2$  stable from  $w$  to  $x$  with the  $\mathcal{L}_2$  gain inequality given by

$$\begin{aligned}
\int_{\delta_{k+1}^c}^{\delta_{k+1}^a} \dot{V} dt &\leq -\beta^2 \int_{\delta_{k+1}^c}^{\delta_{k+1}^a} \|x(t)\|_2^2 dt \\
&+ \Psi^2 \int_{\delta_{k+1}^c}^{\delta_{k+1}^a} \|w(t)\|_2^2 dt + \psi^2 + \xi_k \tau'.
\end{aligned}$$

where the induced gain  $\Psi$  is

$$\begin{aligned}
\Psi &= \frac{1}{\alpha} \left[ \alpha^2 \gamma^2 + 4 \|\sqrt{MB_2}\|_2^2 (e^{\alpha \tau'} - 1)^2 \right. \\
&\quad \left. + \|\sqrt{MB_2}\|_2^2 (e^{2\alpha \tau'} - 1)(e^{2\alpha(\bar{\tau} - \tau')} - 1) \right]^{1/2},
\end{aligned} \quad (21)$$

and the additional term  $\psi$  is

$$\begin{aligned}
\psi &= \frac{\|\sqrt{MB_2}\|_2}{\alpha} \\
&\times \left[ (e^{2\alpha \tau'} - 1)(e^{2\alpha(\bar{\tau} - \tau')} - 1) \int_{\delta_k}^{\delta_{k+1}^c} \|w(s)\|_2^2 ds \right]^{1/2}.
\end{aligned} \quad (22)$$

**Remark 1.** Additional term  $\psi$  is a result of the error accumulated during  $[\delta_k, \delta_{k+1}^c]$ , as depicted in the last term of (11). This additional term and  $\xi_k \tau'$  are bounded and just add to the upper-bound on  $\dot{V}$  in  $\mathcal{L}_2$  gain inequality.

### 3.1. Triggering time computation

The computation is based on the idea to find the time period  $\tau_k$ , which satisfies inequality (8), i.e.,

$$\|\sqrt{M}e_{k+1}^k\|_2 = \mu(x(k)). \quad (23)$$

Based on this idea, the theorem is now presented, which gives  $\tau_k: \mathbb{R}^n \rightarrow \mathbb{R}^+$  as a function of the state  $x(k)$ , i.e., the ST scheme which guarantees finite-gain  $\mathcal{L}_2$  stability from  $w$  to  $x$  for sampled-data system (3).

**Theorem 4.** Consider sampled-data system (3) with Assumptions 1 and 2. Let

- $\beta \in (0, 1)$  be such that  $M$  (defined in (7)) has full rank, and
- the bounded constants  $\sigma \in (0, 1]$ ,  $\underline{\tau}$ ,  $\bar{\tau} \in \mathbb{R}^+$ .

If for any  $k \in \mathbb{Z}^+$

- the initial condition is  $\delta_0 = 0$ , and
- $(k+1)$ th release time satisfies

$$\delta_{k+1} = \delta_k + \max\{\underline{\tau}, \min\{\bar{\tau}, \sigma \tau_k(x(k))\}\}, \quad (24)$$

where  $\tau_k(x(k)): \mathbb{R}^n \rightarrow \mathbb{R}^+$  is defined as

$$\tau_k(x(k)) = \begin{cases} \frac{1}{\alpha} \ln \left( 1 + \frac{\alpha \mu(x(k))}{2\mu_0(x(k))} \right), & x(k) \neq 0 \\ \infty, & x(k) = 0, \end{cases} \quad (25)$$



then system (3) is finite-gain  $\mathcal{L}_2$  stable from  $w$  to  $x$ .

**Remark 2.** Adaptive  $\sigma$  multiplier can also be considered which depends on the amount of disturbance in previously sampled states.

### 3.2. System's Overall State Indicator (SOSI)

As mentioned earlier, the first level controller is responsible for sending next triggering time and SOSI to the second level controller (NM) for PBS. The factors for selection of SOSI are:

- denied transmission requests,
- distance of trajectories from set-point or equilibrium  $\|x(k) - x_e(k)\|_2$ , where  $x_e(k)$  is the equilibrium-point state at  $k$ , and
- magnitude of the disturbance, which can be estimated by a disturbance observer/estimator.

Let  $\mathcal{A}_k^j$ , denoting the SOSI of  $j$ th system where  $j \in \{1, \dots, N\}$ , be given as

$$\mathcal{A}_k^j = m^j \times (\|x^j(k) - x_e^j(k)\|_2), \quad (26)$$

where  $m^j$  is the appropriate weight used to set priority of  $j$ th system. For instance, the monitoring nodes in the network can be assigned low weights relative to the sensing nodes (control loops). Also, the systems which are expected to face disturbance or those which need more attention can be assigned higher weights.

This information, along with the next sampling time, is sent to the NM which computes the *relative* SOSI ( $\mathcal{R}_k^j$ ) of each control loop as

$$\mathcal{R}_k^j = \frac{\mathcal{A}_k^j}{\sum_{q=1}^N \mathcal{A}_k^q} + F_m^j, \quad (27)$$

where  $F_m^j$  denotes the flag indicating previously missed transmission, given as

$$F_m^j = \begin{cases} 0 & \text{if transmission was allowed} \\ 1 & \text{if transmission was denied.} \end{cases} \quad (28)$$

Note that the third factor is not included in the calculation of  $\mathcal{A}_k^j$ , because it demands a disturbance observer which translates into more computational cost. Instead by using the distance of state trajectories from their set-points, disturbance is also accounted because more disturbance results in larger difference between the actual state and its equilibrium value.

## 4. Second level: network manager

The slotted mode of IEEE 802.15.4 wireless networking protocol with modified NM and superframe structures is considered. Details of the said protocol are left due to limited space and can be found in [17]. The motivation for the modifications comes mainly from the use of ST strategy, which does not require the controllers to “contend” for transmission slot due to the predicted triggering times, hence eliminating the need for Contention Access Period

(CAP). This knowledge allows the scheduler to pre-schedule the transmission slots for the next superframe. In addition, as it will be seen in the forthcoming text and simulation results, significant energy savings can be achieved at the battery-powered sensor nodes at the expense of slightly increased computational load at the mains powered NM.

### 4.1. Superframe

In the modified superframe structure, as shown in Fig. 4, the CAP is eliminated and the active and inactive portions are distributed. This allows the systems to get their states at any time during the beacon interval, unlike “fixed” time slots placed in the Contention Free Period (CFP). A superframe can allow at most  $N_{max}$  transmissions each of duration  $\Delta_s$ .

The constraints that govern the choice of  $\tau$  and  $\bar{\tau}$  are imposed by the physical layer of the protocol and plant dynamics. Specifically,

- $\min BI \leq \tau \leq \frac{1}{5\lambda_{min}}$ ,
- $\min BI \leq BI \leq \max BI$ ,
- $\bar{\tau} \leq \max BI$ ,

where  $\lambda_{min}$  denotes the dominant pole of the fastest plant among the participating systems, and  $\min BI$  and  $\max BI$  represent the minimum and maximum values of BI, respectively, corresponding to the constraint  $0 \leq \text{Beacon Order (macBO)} \leq 14$  imposed by the original protocol [17] as

$$BI = aBaseSFDuration \times 2^{\text{macBO}}, \quad (29)$$

with  $aBaseSFDuration \triangleq SFD \equiv \frac{\text{No. of symbols}}{\text{Symbol rate}}$ .

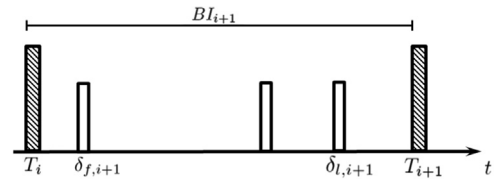


**Fig. 4.** Modified superframe structure. The duration is denoted as  $BI_{i+1}$ . Active period includes a beacon packet and three slots for transmission; remaining time constitutes the inactive period. Each slot is of duration  $\Delta_s$ .

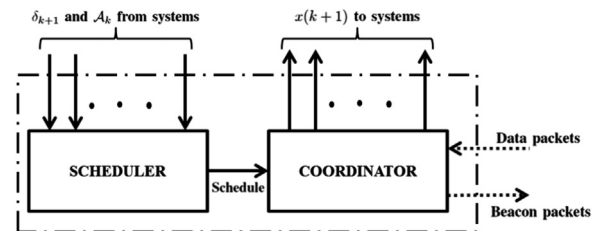


**Fig. 5.** Modified structure of the network manager. Solid line: wired connections; dotted line: wireless link.

#### 4.2. Network manager

The NM has wired connection with the ST controllers and communicates over a wireless link with the sensor nodes. The proposed NM structure appends a scheduler module with the Personal Area Network (PAN) coordinator as shown in Fig. 5. The coordinator transmits beacon packet at the start of each super-frame.

The beacon format contains separate field (comprising a fixed amount of bits allocated) for each sensor node, and one field for beacon interval. The field for sensor node is further composed of a flag and some bits to represent the triggering time. If a node is scheduled for the next beacon interval its flag will be raised, and the corresponding triggering time will be stored in respective field. On the other hand, if a sensor node is not scheduled for the next interval its flag will be low. This enables each sensor node to sleep until its transmission time, transmit the state information in the assigned slot, and sleep again until the next beacon transmission. Note that this flag is not the same as  $F_m^i$ .

After sampling the states of their systems in the assigned slots, the sensor nodes transmit this information over the wireless network to the coordinator, which delivers this information to respective controllers. Each controller computes  $\delta_{k+1}$  and  $\mathcal{A}_k$  (only necessary if  $N > N_{max}$ ), and sends this information to the scheduler over the wired connection. The scheduler keeps storing this information in a buffer until it receives from all the controllers scheduled for that particular beacon interval, and then starts the scheduling algorithm. The NM performs following tasks:

- Ensures that no two transmissions overlap in the next superframe.
- If  $N > N_{max}$ , then implements PBS algorithm.
- Keeps track of the slow systems and places their transmission slots in appropriate superframe. This way, the need to sample every system in each superframe is eliminated.
- Provides the coordinator with a transmission schedule.

**Remark 3.** To avoid overlap of transmissions in case two systems want the same slot, the NM schedules the sampling times in consecutive slots, i.e., one slot-duration apart. This does not have a significant effect on stability, owing to a very small duration of the slot (typically around 1 ms) as compared to the sampling time.

After getting the scheduling information, the coordinator forms a beacon packet and broadcasts it to the sensors.

**Assumption 3.** It is assumed that,

- all the controllers have knowledge of the initial state,  $x(0)$ , of their respective systems,
- the scheduler takes  $\zeta \leq \bar{\zeta} \in \mathbb{R}^+$  units of time for all computations during a superframe,
- a sensor node requires only one slot duration to transmit the whole state information,
- beacon packet requires only one slot duration, and

- $\Delta_s$  includes inter-frame spacing (IFS) (see [17]).

#### 4.3. Modified protocol

Given the predicted triggering time of each system, the length of next SF is computed as  $Bl_{i+1} = \delta_{f,i+1} - T_i - \Delta_s + N_{max}\Delta_s + laP$ , where  $\delta_{f,i+1}$  is the first system which will transmit in the next SF, and  $laP$  denotes the inactive period which will allow the scheduler ample time to construct the next SF and economize energy. In order to ensure schedulability of the first system of next SF in worst-case scenario, whereby that system's predicted triggering time might be  $\underline{\tau}$ , the duration  $N_{max}\Delta_s + laP \leq \underline{\tau} - \Delta_s$ . This results in

$$Bl_{i+1} = \delta_{f,i+1} - T_i - 2\Delta_s + \underline{\tau} \triangleq b. \quad (30)$$

The proposed protocol has two parts, depending upon the number of attached nodes. If the number of nodes is not more than the maximum number of available slots, i.e.,  $N \leq N_{max}$ , then the NM does not require PBS algorithm. Initially, all the controllers use initial states to compute the next triggering times. This information is used by the scheduler to schedule the first superframe starting at  $T_0 = 0$ , and compute its duration following (30) as  $Bl_1 = \delta_{f,1} - T_0 - 2\Delta_s + \underline{\tau}$ , where  $\delta_{f,1}$  denotes the first system which will transmit in the first superframe. Coordinator broadcasts first beacon packet at  $T_0$ , which contains triggering times for all the nodes and the beacon interval  $Bl_1$ . For any superframe  $i$ , the scheduler computes

$$\delta_{l,i+1} - T_i + \Delta_s \triangleq a, \quad (31)$$

besides  $b$ , where  $\delta_{l,i+1}$  denotes the last system which will transmit in the next superframe. The scheduler then compares  $a$  and  $b$ ; if  $a \leq b$  then all the nodes are allowed to transmit in the next superframe, otherwise the nodes for which the next triggering time falls in the next superframe duration are allowed to transmit, and the remaining nodes' slots are placed in the appropriate future superframe. The algorithm is given as follows:

##### Algorithm 1.

```

For  $N \leq N_{max}$ :
Initialization
1.  $i = 0$  and  $k = 0$ .
End Initialization
2. At  $\delta_k^j$  in  $i$ -th superframe, scheduler gets  $\delta_{k+1}^j$  for those
   systems which transmit in  $Bl_i$ ;
3. Wait until  $\delta_{l,i}$ ;
4. Compute (30) and (31);
   If  $a \leq b$  then
5.   All the nodes are allowed transmission in  $Bl_{i+1}$ ;
6.   Increment  $i$  and  $k$  by one;
7.   GOTO 2;
   else
8.   The nodes with  $\delta_{k+1} \in [T_i + \Delta_s, T_{i+1})$  are allowed
      transmission in  $Bl_{i+1}$ ;
9.   Increment  $i$ ;
10.  Increment  $k$  for those systems which transmit in
       $Bl_{i+1}$ ;
11.  GOTO 2;
   end
end

```

Since the algorithm only ensures optimal usage of communication resources while assigning transmission slots to the systems according to their computed triggering times, all the systems will be finite-gain  $\mathcal{L}_2$  stable.

In case the number of systems exceeds the maximum number of transmission slots, i.e.,  $N > N_{\max}$ , the scheduler is provided with  $\mathcal{A}_k$  (26) from each controller besides  $\delta_{k+1}$ . The scheduler then uses this information to schedule the transmission slots according to PBS. In PBS, the priorities are assigned according to  $\mathcal{R}_k$  (27) of each system such that the system with highest  $\mathcal{R}_k$  is guaranteed transmission slot in the next superframe. The remaining nodes for which the transmission is denied are assigned new triggering times as

$$\delta_{\text{new}} = \delta_{l,k+1} + \Delta_s + \tau, \quad (32)$$

and their missed-superframe flag  $F_m$  (28) are also incremented. Note that the value of  $F_m$  reveals the number of consecutively missed superframes of respective system. A sketch of the algorithm is given as follows:

#### Algorithm 2.

```

For  $N > N_{\max}$ :
Initialization
1.  $i=0$  and  $k=0$ ;
2. Clear all flags i.e.,  $F_m=0$ .
End Initialization
3. At  $\delta_k^j$  in  $i$ -th superframe, scheduler gets  $\delta_{k+1}^j$  and  $\mathcal{A}_k^j$  for
   those systems which transmit in  $Bl_i$ ;
4. Wait until  $\delta_{ij}$ ;
5. Call PBS function;
6. Compute (30) and (31);
   If  $a \leq b$  then
7.   The first  $N_{\max}$  nodes with highest  $\mathcal{R}_k^j$  values transmit
      in  $Bl_{i+1}$ ;
8.   Increment  $i$ ;
9.   Increment  $k$  for those systems which transmit in
       $Bl_{i+1}$ ;
10.  GOTO 3;
   else
11.  The nodes with  $\delta_{k+1} \in [T_i + \Delta_s, T_{i+1})$  transmit in  $Bl_{i+1}$ ;
12.  Increment  $i$ ;
13.  Increment  $k$  for those systems which transmit in
       $Bl_{i+1}$ ;
14.  GOTO 3;
   end
Function: PBS
15. Compute (27);
16. The first  $N_{\max}$  nodes with highest  $\mathcal{R}_k^j$  values are allowed
   transmission in  $Bl_{i+1}$ ;
17. Clear  $F_m$  for systems which will transmit in  $Bl_{i+1}$ ;
18. The remaining nodes are assigned consecutive
   transmission slots starting from (32);
19. Increment  $F_m$  for the remaining nodes;
20. Return;
end

```

**Remark 4.** For this paper,  $N \leq N_{\max} + 1$  is considered. A detailed analysis of the bound on  $N$  will be considered in future work.

**Theorem 5.** Consider  $N$  sampled-data systems represented by (3), with Assumptions 1 and 2, which share a common wireless communication medium, under Assumption 3, to close their feedback loops; with the inequalities and constants defined in Theorem 3. The communication medium

**Table 1**  
Parameters.

Parameter	Value
$m_b$	1
$M_c$	10
$l$	3
$x_o$	$[0.98 \ 0 \ 0.2 \ 0]^T$
$\beta$ , Eq. (7)	0.3
$\gamma$ , Eq. (2)	200
$\sigma$ , Eq. (24)	1
$\lambda_{\min}$	1.8257
$\tau$	0.106
$\bar{\tau}$	0.45
$m$ , Eq. (26)	1 (Sys1); 12 (Sys2); 5 (Sys3)

has limited number of transmission slots  $N_{\max}$ ,  $N > N_{\max}$ . If the communication protocol applies Algorithm 2, then all the control loops are finite-gain  $\mathcal{L}_2$  stable from  $w$  to  $x$  with a bounded induced gain.

## 5. Simulation results and discussion

Simulation results of the application of the above defined scheme are now presented for three identical inverted pendulum over a moving cart systems represented by (3), with state vector  $x = [y \ \dot{y} \ \theta \ \dot{\theta}]^T$ , where  $y$  and  $\theta$  denote the cart's position and bob's angle, respectively. The system matrices are given as

$$A = \begin{bmatrix} 0 & 1 & 0 & 0 \\ 0 & 0 & -\frac{m_b g}{M_c} & 0 \\ 0 & 0 & 0 & 1 \\ 0 & 0 & \frac{g}{l} & 0 \end{bmatrix}; \quad B_1 = \begin{bmatrix} 0 \\ \frac{1}{M_c} \\ 0 \\ -\frac{1}{M_c l} \end{bmatrix}; \quad B_2 = \begin{bmatrix} 1 \\ 1 \\ 1 \\ 1 \end{bmatrix}, \quad (33)$$

where  $m_b$  is bob's mass,  $M_c$  denotes cart's mass,  $l$  is the length of the pendulum, and  $g$  is gravitational acceleration. The values of  $N_{\max} = 4$  for Algorithm 1 and  $N_{\max} = 2$  for Algorithm 2.  $\Delta_s = (\text{Number of symbols in one slot}) / (\text{Symbol rate})$ , where the values given in Tables 51 and 66 of [17] are 60 symbols per slot and 40 ksymbols/s (for 915 MHz band), respectively. The values of all the parameters are given in Table 1. The choice of weights for (26) is made such that the system experiencing disturbance gets high priority. In this simulation, systems 2 and 3 experience  $w(t)$  as

$$\text{System2: } w(t) = 0.1 \text{sgn}(\sin t), \quad 0 \leq t < 10, \\ = 0, \quad \text{otherwise.}$$

$$\text{System3: } w(t) = 0.3(\sin 5t), \quad 0 \leq t < 4, \\ = 0, \quad \text{otherwise.} \quad (34)$$

In order to compare the schemes, two separate measures of duty cycle are introduced. The first one indicates transmission time, and the second gives listening period of the sensor nodes. The reason is the difference in power consumed by the sensor nodes in transmission and reception modes, which is also indicated in [29]. The expressions are given as  $DC_{tx} = (\text{No. of transmissions in } Bl_i \times \Delta_s) / (Bl_i)$  and  $DC_{rx} = (\Delta_s) / (Bl_i)$ , where  $\Delta_s$  denotes the time duration of transmission slot or beacon packet, because it is assumed



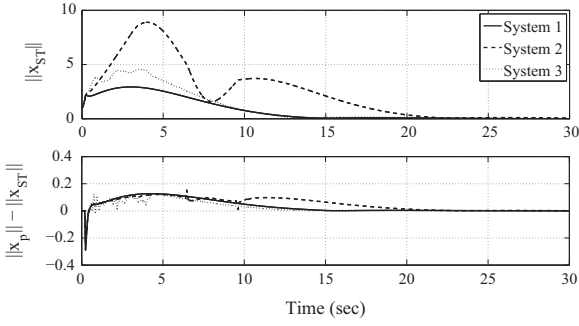


**Fig. 6.** System states. Top:  $\|x_{ST}(t)\|$  for Algorithm 1; bottom:  $\|x_p(t)\| - \|x_{ST}(t)\|$ , where  $x_p(t)$  denotes states for periodic implementation.

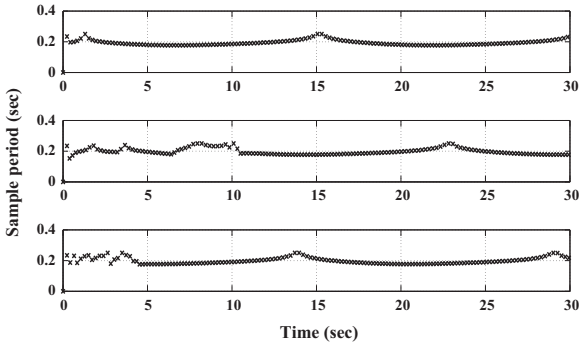


**Fig. 7.** ST events. Top: System 1, middle: System 2, bottom: System 3.

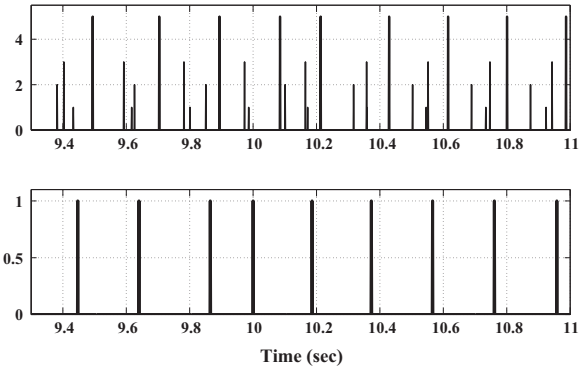


**Fig. 8.** Snapshot of transmissions,  $N_{max}=4$ . Top: beacon packets and transmissions for Systems 1, 2, and 3 are scaled as 5, 1, 2, and 3, respectively; bottom: duty cycle of the scheduler.

that each transmission from the sensor nodes, and beacon packet transmission take one slot to complete (Assumption 3).

**Algorithm 1:** Results of Algorithm 1 are compared against periodic implementation of the same systems over original IEEE 802.15.4 protocol for which  $BO=4$  and  $\tau=0.192$  s for all the systems, which are assigned consecutive GTs in every superframe, and  $N_{max}=4$ . The results are given in Figs. 6–8. All the systems are stabilized within 30 s and the difference between the states in Fig. 6 shows that the fixed sampling time in periodic implementation results in higher magnitude in transient phase as compared with the adaptive ST times.

**Table 2**

Comparison of three implementations for simulation time of 30 s. The periodic scheme uses  $BO=4$  and  $\tau=0.192$ . Tx  $j$ : number of transmissions from  $j$ -th system; SF: number of superframes.

Imp.	Tx1	Tx2	Tx3	SF	Av. $DC_{tx}$ (%)	Av. $DC_{rx}$ (%)
Periodic	474	474	474	158	14.22	1.58
Algo. 1	150	152	152	173	4.54	1.73
Algo. 2	93	153	93	184	3.39	1.84

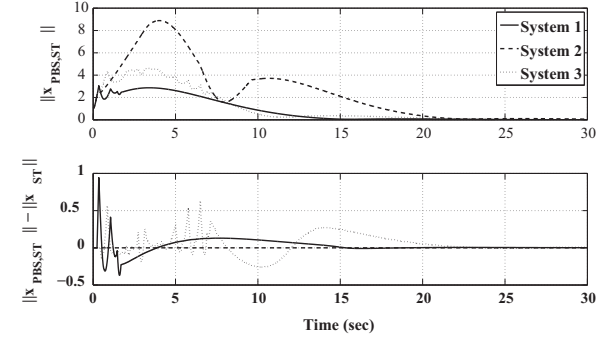


**Fig. 9.** System states. Top:  $\|x_{PBS,ST}(t)\|$  for Algorithm 2; bottom:  $\|x_{PBS,ST}(t)\| - \|x_{ST}(t)\|$ , where  $\|x_{PBS,ST}(t)\|$  denotes the states due to PBS algorithm.

Fig. 7 shows that the ST scheme adjusts triggering times according to the disturbance encountered by the system. Moreover, the assigned triggering times to all the systems follow the bounds  $\tau$  and  $\bar{\tau}$ . A snapshot of the transmissions is shown in Fig. 8, which demonstrates the generation of superframes with variable duration, and transmission from the systems. It can be seen that some of the superframes do not contain transmissions from all three systems, which supports the communication-saving claim of the proposed algorithm. In addition, the operation of the scheduler is also shown which starts its execution after the last transmission in each superframe.

As reported in Table 2, the periodic scheme demands more transmissions, translating into greater bandwidth and energy usage as compared with the proposed ST implementation in Algorithm 1. The results indicate a 68% decrease in average  $DC_{tx}$  and 9.5% increase in average  $DC_{rx}$ , which show that despite a slight increase in the listening period of the nodes, the transmission duration has decreased significantly.

**Algorithm 2:** Now the results of Algorithm 2 and Algorithm 1 are compared. Fig. 9 (top) shows more variations in the transient periods of systems 1 and 3 as compared with system 2. Also, the difference in states for both algorithms (bottom) shows variations only for systems 1 and 3. This is due to the choice of weights (Table 1) for PBS algorithm which give highest priority to system 2 as compared with systems 1 and 3.

Due to the same reason, Fig. 10 shows that the event times for system 2 are in the range of 0.15–0.25 s and that for systems 1 and 3 are in the range of 0.2–0.45 s, i.e., system 2 is given more attention as compared with systems 1 and 3. Table 2 reveals the same fact where the number of ST events reduces from 150 and 152 to 93 for

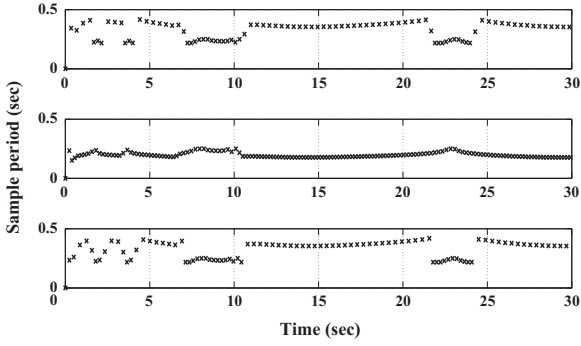


Fig. 10. ST events. Top: System 1, middle: System 2, bottom: System 3.

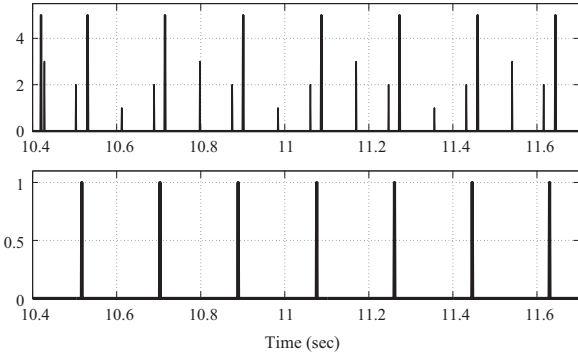


Fig. 11. Snapshot of transmissions,  $N_{max}=2$ . Top: beacon packets and transmissions for Systems 1, 2 and 3 are scaled as 5, 1, 2, and 3, respectively, bottom: duty cycle of the scheduler.

systems 1 and 3, respectively. Also, a significant decrease of 25% in  $DC_{rx}$  as compared with Algorithm 1 can be observed at the expense of a slight increase of 6.4% in  $DC_{rx}$ .

Note that the event times assigned by NM to systems 1 and 3 are larger than  $\bar{\tau}$  due to limited number of transmission slots, and these systems are still stable with increased variation in state trajectories, which conforms with the results of Theorem 3. Additionally, Fig. 10 shows that when system 2 demands less number of samples, the other two systems are allowed to have more frequent transmissions, for instance between 6 and 11 s. This shows that PBS algorithm works as intended and accommodates the systems according to the assigned priorities and transmission requirements.

Fig. 11 shows more frequent transmissions of system 2, variable beacon intervals, and a maximum of two transmissions allowed in each superframe.

## 6. Conclusion

A two-level design for NCSs is presented by employing ST  $\mathcal{H}_\infty$  controller over modified IEEE 802.15.4 protocol. First level is composed of ST based  $\mathcal{H}_\infty$  controller for each system, which guarantees finite-gain  $\mathcal{L}_2$  stability, and second level comprises the modified IEEE protocol. These modifications are introduced to the MAC layer, given by two algorithms depending upon the number of participating control loops and maximum number of transmission slots.

The main advantages of the proposed methodology over existing literature, which motivate the practical use of the theoretic study, are the improvement in energy efficiency of the said protocol due to the modifications, and provision of adding one more control loop than the maximum number of transmission slots while guaranteeing control performance. Additionally, the proposed methodology requires less computational power as compared with [19], because it pre-schedules the next beacon interval without computing the disturbance estimate and two-steps ahead triggering time.

The simulations for Algorithm 1 indicate a 68% decrease in the average transmission duty cycle of the sensor nodes against periodic implementation over the original IEEE protocol, with a slight increase of 9.5% in the average reception duty cycle. PBS based Algorithm 2 shows a 25% decrease in average transmission duty cycle as compared with the first algorithm, with an increase of 6.4% in the reception duty cycle.

Adaptive weights,  $m^j$  for SOSI, which adjust according to the disturbance experienced by the system, and practical implementation of the presented methodology will be considered as topics of future research.

## Appendix

### Proof of Lemma 2

**Proof.** Case 1: Let  $\Omega = \{t \in [\delta_k, \delta_{k+1}): \|\sqrt{M}e_t^k\|_2 = 0\}$ , i.e., the time for which error is zero. The time derivative of  $\|\sqrt{M}e_t^k\|_2$  for  $t \in [\delta_k, \delta_{k+1}) \setminus \Omega$  satisfies

$$\begin{aligned} \frac{d}{dt} \|\sqrt{M}e_t^k\|_2 &\leq \|\sqrt{M}\dot{e}_t^k\|_2 = \|\sqrt{M}\dot{x}(t)\|_2 \\ &= \|\sqrt{M}(Ae_t^k + (A - B_1B_1^T)P)x(k) + B_2w(t)\|_2 \\ (\because x(t) &= e_t^k + x(k)) \\ &= \|\sqrt{M}A\sqrt{M}^{-1}\sqrt{M}e_t^k + \sqrt{M}\bar{A}x(k) + \sqrt{M}B_2w(t)\|_2 \\ &\leq \alpha \|\sqrt{M}e_t^k\|_2 + \mu_0(x(k)) + \|\sqrt{M}B_2\|_2 \|w(t)\|_2. \end{aligned} \quad (35)$$

Solving the above differential inequality with  $\|\sqrt{M}e_k^k\|_2 = 0$  for  $t = \delta_k$ , we get

$$\begin{aligned} \|\sqrt{M}e_t^k\|_2 &\leq \frac{\mu_0(x(k))}{\alpha} (e^{\alpha(t-\delta_k)} - 1) \\ &\quad + \int_{\delta_k}^t e^{\alpha(t-s)} \|\sqrt{M}B_2\|_2 \|w(s)\|_2 ds, \end{aligned}$$

which gives the error bound for  $t \in (\delta_k, \delta_{k+1})$ .

Case 2: Refer to Fig. 3. For duration  $t \in (\delta_k, \delta_{k+1}^a)$ , the closed-loop system is given as

$$\dot{x}(t) = \bar{A}x(k) + B_2w(t). \quad (36)$$

Divide  $t \in (\delta_k, \delta_{k+1}^a)$  into two parts,  $t_1 \in (\delta_k, \delta_{k+1}^c)$  and  $t_2 \in (\delta_{k+1}^c, \delta_{k+1}^a)$ . Let  $\Omega_1 = \{t_1 \in (\delta_k, \delta_{k+1}^c): \|\sqrt{M}e_t^k\|_2 = 0\}$  i.e., the time at which error goes to zero. The error bound for  $t_1 \in (\delta_k, \delta_{k+1}^c) \setminus \Omega_1$  satisfies the same inequality as (10).

Let  $\Omega_2 = \{t_2 \in [\delta_{k+1}^c, \delta_{k+1}^a): \|\sqrt{M}e_t^k\|_2 = 0\}$ , then

$$\frac{d}{dt} \|\sqrt{M}e_t^k\|_2 \leq \alpha \|\sqrt{M}e_t^k\|_2 + \mu_0(x(k)) + \|\sqrt{M}B_2\|_2 \|w(t)\|_2.$$

Solving the above differential inequality with

$$\begin{aligned} \|\sqrt{M}e_{k+1}^k\|_2 &\leq \frac{\mu_0(x(k))}{\alpha} \left( e^{\alpha(\delta_{k+1}^c - \delta_k)} - 1 \right) \\ &\quad + \int_{\delta_k}^{\delta_{k+1}^c} e^{\alpha(\delta_{k+1}^c - s)} \|\sqrt{M}B_2\|_2 \|w(s)\|_2 ds, \end{aligned} \quad (37)$$

obtained from (10) at  $t = \delta_{k+1}^c$ , we get

$$\begin{aligned} \|\sqrt{M}e_t^k\|_2 &\leq \frac{\mu_0(x(k))}{\alpha} \left( e^{\alpha(t - \delta_k)} - 1 \right) \\ &\quad + \int_{\delta_{k+1}^c}^t e^{\alpha(t-s)} \|\sqrt{M}B_2\|_2 \|w(s)\|_2 ds \\ &\quad + e^{\alpha(t - \delta_{k+1}^c)} \int_{\delta_k}^{\delta_{k+1}^c} e^{\alpha(\delta_{k+1}^c - s)} \|\sqrt{M}B_2\|_2 \|w(s)\|_2 ds, \end{aligned}$$

which gives the error bound for  $t \in [\delta_{k+1}^c, \delta_{k+1}^a]$ .  $\square$

### Proof of Theorem 3

**Proof.** A similar methodology as [14] is followed.

**Case 1:** From Lemma 2 it is known that (10) holds for  $t \in (\delta_k, \delta_{k+1})$ . Squaring both sides of (10), we get

$$\begin{aligned} \|\sqrt{M}e_t^k\|_2^2 &\leq 4 \left( \frac{\mu_0(x(k))}{\alpha} \left( e^{\alpha(t - \delta_k)} - 1 \right) \right)^2 \\ &\quad + 4 \left( \int_{\delta_k}^t e^{\alpha(t-s)} \|\sqrt{M}B_2\|_2 \|w(s)\|_2 ds \right)^2. \end{aligned} \quad (38)$$

Substituting (38) in (6) (Lemma 1), we get

$$\begin{aligned} \dot{V} &\leq -\beta^2 \|x(t)\|_2^2 + \gamma^2 \|w(t)\|_2^2 - x^T(k)Nx(k) \\ &\quad + 4 \left( \frac{\mu_0(x(k))}{\alpha} \left( e^{\alpha(t - \delta_k)} - 1 \right) \right)^2 \\ &\quad + 4 \left( \int_{\delta_k}^t e^{\alpha(t-s)} \|\sqrt{M}B_2\|_2 \|w(s)\|_2 ds \right)^2, \end{aligned} \quad (39)$$

for all  $t \in (\delta_k, \delta_{k+1})$ . For notational convenience, let

$$\mathcal{I}(t) = \int_{\delta_k}^t e^{\alpha(t-s)} \|\sqrt{M}B_2\|_2 \|w(s)\|_2 ds. \quad (40)$$

Integrating both sides of (39) for all  $t \in (\delta_k, \delta_{k+1})$ ,

$$\begin{aligned} \int_{\delta_k}^{\delta_{k+1}} \dot{V} dt &\leq -\beta^2 \int_{\delta_k}^{\delta_{k+1}} \|x(t)\|_2^2 dt + \gamma^2 \int_{\delta_k}^{\delta_{k+1}} \|w(t)\|_2^2 dt \\ &\quad - \int_{\delta_k}^{\delta_{k+1}} x^T(k)Nx(k) dt + \int_{\delta_k}^{\delta_{k+1}} 4\mathcal{I}(t)^2 dt \\ &\quad + \int_{\delta_k}^{\delta_{k+1}} 4 \left( \frac{\mu_0(x(k))}{\alpha} \left( e^{\alpha(t - \delta_k)} - 1 \right) \right)^2 dt. \end{aligned} \quad (41)$$

Evaluating the last term, we get

$$\begin{aligned} &\int_{\delta_k}^{\delta_{k+1}} 4 \left( \frac{\mu_0(x(k))}{\alpha} \left( e^{\alpha(t - \delta_k)} - 1 \right) \right)^2 dt \\ &= \frac{2\mu_0^2}{\alpha^3} [2\alpha(\delta_{k+1} - \delta_k) - 4e^{\alpha(\delta_{k+1} - \delta_k)} + e^{2\alpha(\delta_{k+1} - \delta_k)} + 3] \\ &\leq \int_{\delta_k}^{\delta_{k+1}} x^T(k)Nx(k) dt, \end{aligned} \quad (42)$$

where the inequality is obtained from (14) which is

enforced by the choice of  $\delta_{k+1}$ . Substituting (42) into (41),

$$\begin{aligned} \int_{\delta_k}^{\delta_{k+1}} \dot{V} dt &\leq -\beta^2 \int_{\delta_k}^{\delta_{k+1}} \|x(t)\|_2^2 dt + \gamma^2 \int_{\delta_k}^{\delta_{k+1}} \|w(t)\|_2^2 dt \\ &\quad + \int_{\delta_k}^{\delta_{k+1}} 4\mathcal{I}(t)^2 dt. \end{aligned} \quad (43)$$

Using Cauchy–Schwarz inequality

$$\left( \int_a^b X(t)Y(t) dt \right)^2 \leq \left( \int_a^b X^2(t) dt \right) \left( \int_a^b Y^2(t) dt \right), \quad (44)$$

to bound the integral in the last term of (43), we get

$$\begin{aligned} \int_{\delta_k}^{\delta_{k+1}} 4\mathcal{I}(t)^2 dt &\leq \frac{4\|\sqrt{M}B_2\|_2^2}{\alpha^2} (e^{\alpha(\delta_{k+1} - \delta_k)} - 1)^2 \\ &\quad \int_{\delta_k}^{\delta_{k+1}} \|w(s)\|_2^2 ds. \end{aligned} \quad (45)$$

Applying the bounds given in (13), the upper and lower bounds on (43) are obtained as

$$\begin{aligned} &-\beta^2 \int_{\delta_k}^{\delta_{k+1}} \|x(t)\|_2^2 dt + \left[ \gamma^2 + \frac{4\|\sqrt{M}B_2\|_2^2}{\alpha^2} (e^{\alpha \tau} - 1)^2 \right] \\ &\quad \int_{\delta_k}^{\delta_{k+1}} \|w(s)\|_2^2 ds \leq \int_{\delta_k}^{\delta_{k+1}} \dot{V} dt \leq \\ &-\beta^2 \int_{\delta_k}^{\delta_{k+1}} \|x(t)\|_2^2 dt + \left[ \gamma^2 + \frac{4\|\sqrt{M}B_2\|_2^2}{\alpha^2} (e^{\alpha \bar{\tau}} - 1)^2 \right] \\ &\quad \int_{\delta_k}^{\delta_{k+1}} \|w(s)\|_2^2 ds. \end{aligned} \quad (46)$$

Summing the above inequality for all  $k \in \mathbb{Z}^+$ , we get

$$\begin{aligned} &-\beta^2 \int_0^\infty \|x(t)\|_2^2 dt + \underline{\Gamma}^2 \int_0^\infty \|w(s)\|_2^2 ds \leq \int_0^\infty \dot{V} dt \leq \\ &-\beta^2 \int_0^\infty \|x(t)\|_2^2 dt + \bar{\Gamma}^2 \int_0^\infty \|w(s)\|_2^2 ds, \end{aligned} \quad (47)$$

where  $\underline{\Gamma}$  and  $\bar{\Gamma}$  are defined in (16). Inequality (47) shows that sampled-data system (3) is finite-gain  $\mathcal{L}_2$  stable from  $w$  to  $x$  with an induced gain bounded between  $\underline{\Gamma}$  and  $\bar{\Gamma}$ .

**Case 2:** Following the similar analysis as in case 1, squaring both sides of (11), we get

$$\begin{aligned} \|\sqrt{M}e_t^k\|_2^2 &\leq 4 \left( \frac{\mu_0(x(k))}{\alpha} \left( e^{\alpha(t - \delta_k)} - 1 \right) \right)^2 \\ &\quad + 4 \left( \int_{\delta_{k+1}^c}^t e^{\alpha(t-s)} \|\sqrt{M}B_2\|_2 \|w(s)\|_2 ds \right)^2 \\ &\quad + 4 \left( e^{\alpha(t - \delta_{k+1}^c)} \int_{\delta_k}^{\delta_{k+1}^c} e^{\alpha(\delta_{k+1}^c - s)} \|\sqrt{M}B_2\|_2 \|w(s)\|_2 ds \right)^2. \end{aligned} \quad (48)$$

Substituting (48) in (6), we get

$$\begin{aligned} \dot{V} &\leq -\beta^2 \|x(t)\|_2^2 + \gamma^2 \|w(t)\|_2^2 - x^T(k)Nx(k) \\ &\quad + 4 \left( \frac{\mu_0(x(k))}{\alpha} \left( e^{\alpha(t - \delta_k)} - 1 \right) \right)^2 \\ &\quad + 4 \left( \int_{\delta_{k+1}^c}^t e^{\alpha(t-s)} \|\sqrt{M}B_2\|_2 \|w(s)\|_2 ds \right)^2 \end{aligned}$$

$$+ 4e^{2\alpha(t-\delta_{k+1}^c)} \left( \int_{\delta_k^c}^{\delta_{k+1}^c} e^{\alpha(\delta_{k+1}^c-s)} \|\sqrt{MB_2}\|_2 \|w(s)\|_2 ds \right)^2, \quad (49)$$

for all  $t \in [\delta_{k+1}^c, \delta_{k+1}^a]$ . For notational convenience, let

$$\begin{aligned} \mathcal{I}_1(t) &= \int_{\delta_{k+1}^c}^t e^{\alpha(t-s)} \|\sqrt{MB_2}\|_2 \|w(s)\|_2 ds; \\ \mathcal{I}_2(t) &= \int_{\delta_k^c}^{\delta_{k+1}^c} e^{\alpha(\delta_{k+1}^c-s)} \|\sqrt{MB_2}\|_2 \|w(s)\|_2 ds. \end{aligned} \quad (50)$$

Integrating both sides of (49) for all  $t \in [\delta_{k+1}^c, \delta_{k+1}^a]$

$$\begin{aligned} \int_{\delta_{k+1}^c}^{\delta_{k+1}^a} \dot{V} dt &\leq -\beta^2 \int_{\delta_{k+1}^c}^{\delta_{k+1}^a} \|x(t)\|_2^2 dt + \gamma^2 \int_{\delta_{k+1}^c}^{\delta_{k+1}^a} \|w(t)\|_2^2 dt \\ &\quad - \int_{\delta_{k+1}^c}^{\delta_{k+1}^a} x^T(k)Nx(k) dt + \int_{\delta_{k+1}^c}^{\delta_{k+1}^a} 4\mathcal{I}_1(t)^2 dt \\ &\quad + \int_{\delta_{k+1}^c}^{\delta_{k+1}^a} 4 \left( \frac{\mu_0(x(k))}{\alpha} (e^{\alpha(t-\delta_k)} - 1) \right)^2 dt \\ &\quad + \int_{\delta_{k+1}^c}^{\delta_{k+1}^a} 4e^{2\alpha(t-\delta_{k+1}^c)} \mathcal{I}_2(t)^2 dt. \end{aligned} \quad (51)$$

Evaluating the fifth term, we get

$$\begin{aligned} \int_{\delta_{k+1}^c}^{\delta_{k+1}^a} 4 \left( \frac{\mu_0(x(k))}{\alpha} (e^{\alpha(t-\delta_k)} - 1) \right)^2 dt \\ = \frac{2\mu_0^2}{\alpha^3} [2\alpha(\delta_{k+1}^a - \delta_{k+1}^c) + e^{-2\alpha\delta_k} (e^{\alpha\delta_{k+1}^a} - e^{\alpha\delta_{k+1}^c}) \\ (e^{\alpha\delta_{k+1}^a} + e^{\alpha\delta_{k+1}^c} - 4e^{\alpha\delta_k})]. \end{aligned} \quad (52)$$

Using Taylor series expansion  $e^\delta = 1 + \delta + \mathcal{O}$ , where  $\mathcal{O}$  represents the higher order terms (negligible for small values of  $\delta$ ), we can rewrite (52) as

$$\begin{aligned} \int_{\delta_{k+1}^c}^{\delta_{k+1}^a} 4 \left( \frac{\mu_0(x(k))}{\alpha} (e^{\alpha(t-\delta_k)} - 1) \right)^2 dt &= \frac{4\mu_0^2}{\alpha^2} (\delta_{k+1}^a - \delta_{k+1}^c) \\ &\quad + \frac{2\mu_0^2}{\alpha^2} (1 - 2\alpha\delta_k + \mathcal{O}) (\delta_{k+1}^a - \delta_{k+1}^c + \mathcal{O}) \\ &\quad \times (e^{\alpha\delta_{k+1}^a} + e^{\alpha\delta_{k+1}^c} - 4e^{\alpha\delta_k}) \\ &= \frac{4\mu_0^2}{\alpha^2} (\delta_{k+1}^a - \delta_{k+1}^c) + \frac{2\mu_0^2}{\alpha^2} \\ &\quad \times [(\delta_{k+1}^a - \delta_{k+1}^c) + \mathcal{O} - 2\alpha\delta_k (\delta_{k+1}^a - \delta_{k+1}^c) \\ &\quad - 2\alpha\delta_k \mathcal{O} + (\delta_{k+1}^a - \delta_{k+1}^c) \mathcal{O} + \mathcal{O}] \\ &\quad \times (e^{\alpha\delta_{k+1}^a} + e^{\alpha\delta_{k+1}^c} - 4e^{\alpha\delta_k}) \\ &= \frac{4\mu_0^2}{\alpha^2} (\delta_{k+1}^a - \delta_{k+1}^c) + \frac{2\mu_0^2}{\alpha^2} (\delta_{k+1}^a - \delta_{k+1}^c) \\ &\quad \times [1 + \mathcal{O} - 2\alpha\delta_k - 2\alpha\delta_k \mathcal{O} + \mathcal{O}] (e^{\alpha\delta_{k+1}^a} + e^{\alpha\delta_{k+1}^c} - 4e^{\alpha\delta_k}) \\ &= (\delta_{k+1}^a - \delta_{k+1}^c) \left[ \frac{4\mu_0^2}{\alpha^2} + \frac{2\mu_0^2}{\alpha^2} \mathcal{O} \right]. \end{aligned} \quad (53)$$

where with a slight abuse of notation, we regard the result of all operations on the higher order terms as  $\mathcal{O}$ , and  $\mu_0(x(k))$  is represented as  $\mu_0$ . Evaluating  $\mu_0^2(x(k))$  using (9) gives

$$\begin{aligned} \mu_0^2(x(k)) &= x^T(k) \bar{A}^T \sqrt{M}^T \sqrt{M} \bar{A} x(k) \\ &\leq x^T(k) A^T \sqrt{M}^T \sqrt{M} A x(k) \\ &(\because \bar{A} = A - B_1 B_1^T P \Rightarrow \bar{A} \leq A) \end{aligned}$$

$$\begin{aligned} &\leq x^T(k) \sqrt{M}^T \sqrt{M}^{-T} A^T \sqrt{M}^T \sqrt{M} A \sqrt{M}^{-1} \sqrt{M} x(k) \\ &\leq \alpha^2 x^T(k) M x(k) \\ &(\because \alpha^2 = \sqrt{M}^{-T} A^T \sqrt{M}^T \sqrt{M} A \sqrt{M}^{-1}) \\ &\leq 2\alpha^2 x^T(k) N x(k) \\ &(\because M = 2N - PB_1 B_1^T P \Rightarrow M \leq 2N; \text{ see (7)}) \\ &\leq 2\alpha^2 x^T(k) N x(k). \end{aligned}$$

Substituting this into (53), gives

$$\begin{aligned} \int_{\delta_{k+1}^c}^{\delta_{k+1}^a} 4 \left( \frac{\mu_0(x(k))}{\alpha} (e^{\alpha(t-\delta_k)} - 1) \right)^2 dt \\ \leq (\delta_{k+1}^a - \delta_{k+1}^c) [x^T(k) N x(k) + \xi_k] \\ \leq \int_{\delta_{k+1}^c}^{\delta_{k+1}^a} x^T(k) N x(k) dt + \xi_k (\delta_{k+1}^a - \delta_{k+1}^c). \end{aligned} \quad (54)$$

**Remark 5.** Note that the higher order terms  $\mathcal{O}$  are lumped in the bounded constant  $\xi_k$ .

Substituting (54) into (51) and applying the bound given in Assumption 2, we get

$$\begin{aligned} \int_{\delta_{k+1}^c}^{\delta_{k+1}^a} \dot{V} dt &\leq -\beta^2 \int_{\delta_{k+1}^c}^{\delta_{k+1}^a} \|x(t)\|_2^2 dt + \gamma^2 \int_{\delta_{k+1}^c}^{\delta_{k+1}^a} \|w(t)\|_2^2 dt \\ &\quad + \int_{\delta_{k+1}^c}^{\delta_{k+1}^a} 4\mathcal{I}_1(t)^2 dt \\ &\quad + \int_{\delta_{k+1}^c}^{\delta_{k+1}^a} 4e^{2\alpha(t-\delta_{k+1}^c)} \mathcal{I}_2(t)^2 dt + \xi_k \tau'. \end{aligned} \quad (55)$$

Using (44) and applying bounds given in Assumption 2 on the last two integrals, we get

$$\begin{aligned} \int_{\delta_{k+1}^c}^{\delta_{k+1}^a} \dot{V} dt &\leq -\beta^2 \int_{\delta_{k+1}^c}^{\delta_{k+1}^a} \|x(t)\|_2^2 dt + \xi_k \tau' \\ &\quad + \Psi^2 \int_{\delta_{k+1}^c}^{\delta_{k+1}^a} \|w(t)\|_2^2 dt + \psi^2. \end{aligned} \quad (56)$$

where  $\Psi$  and  $\psi$  are defined in (21) and (22), respectively. Since the terms  $\psi^2$  and  $\xi_k \tau'$  are bounded, the inequality (56) is sufficient to show that the sampled-data system (3) is finite-gain  $\mathcal{L}_2$  stable from  $w$  to  $x$  with an induced gain less than  $\Psi$ .  $\square$

## Proof of Theorem 4

**Proof.** As mentioned in the proof of Theorem 3, the choice of triggering time guarantees  $\mathcal{L}_2$  stability. It will be shown now that ST scheme given by (24) indeed satisfies (12)–(14).

Since the triggering time is lower bounded by  $\tau$ , inequality (12) is satisfied. Furthermore, the upper and lower bounds enforced in (24) show that (13) is also satisfied. For the third inequality i.e., (14), we will show that the expression for  $\tau_k(x(k))$  satisfies the  $\mathcal{L}_2$  stability condition. Specifically, we evaluate the expression  $4 \left( \frac{\mu_0(x(k))}{\alpha} (e^{\alpha(t-\delta_k)} - 1) \right)^2$  at  $t = \delta_{k+1}$ , which is the deterministic part of squared error bound (38). Taking square root

and substituting  $t = \delta_{k+1}$  from (24), we get

$$2 \left( \frac{\mu_0(x(k))}{\alpha} (e^{\alpha(t-\delta_k)} - 1) \right) \leq \mu(x(k)),$$

which shows that the choice of  $\tau_k(x(k))$  renders sampled data system (3) finite-gain  $\mathcal{L}_2$  stable for all  $t \in [\delta_k, \delta_{k+1})$ .

### Proof of Theorem 5

**Proof.** For those  $N_{max}$  systems which are assigned their demanded triggering times, the stability is given in Theorem 3. The remaining systems which are assigned consecutive time slots starting from (32), the stability is given as follows:

The systems which were not allotted time slots in the coming  $BI$ , are now scheduled according to (32), which results in their assigned times as

$$\delta_{k+1}^a = \delta_{lk+1} + \Delta_s + \underline{\tau}. \quad (57)$$

The difference between the assigned time in (57) and the one demanded by the system ( $\delta_{k+1}^s$ ) will be bounded since the right hand side of (57) is constant considering  $\delta_{lk+1}$ , which is a fixed time instant corresponding to the last system to transmit in the next  $BI$ . Hence Assumption 2 holds, and the stability follows directly from Theorem 3, Case 2.  $\square$

### References

- [1] A. Molin, S. Hirche, A bi-level approach for the design of event-triggered control systems over a shared network, *Discrete Event Dyn. Syst.* 24 (2) (2014) 153–171.
- [2] Q.-S. Jia, K.H. Johansson, Guest editorial: event-based control and optimization, *Discrete Event Dyn. Syst.* 24 (2) (2014) 99–102.
- [3] M.S. Mahmoud, A.M. Memon, Aperiodic triggering mechanisms for networked control systems, *Inf. Sci.* 296 (March) (2015) 282–306.
- [4] M. Velasco, P. Martí, J.M. Fuertes, The self-triggered task model for real-time control systems, in: *Proceedings of the 24th IEEE Real-Time Systems Symposium (RTSS03)*, vol. 384, 2003.
- [5] Q. Zhu, B. Xie, Y. Zhu, Controllability and observability of multi-rate networked control systems with both time delay and packet dropout, *Int. J. Innov. Comput., Inf. Control* 11 (February (1)) (2015) 31–42.
- [6] X. Su, L. Wu, P. Shi, Sensor networks with random link failures: distributed filtering for T-S fuzzy systems, *IEEE Trans. Ind. Inf.* 9 (August (3)) (2013) 1739–1750.
- [7] R. Yang, P. Shi, G.-P. Liu, Filtering for discrete-time networked nonlinear systems with mixed random delays and packet dropouts, *IEEE Trans. Autom. Control* 56 (November (11)) (2011) 2655–2660.
- [8] R. Yang, G.-P. Liu, P. Shi, C. Thomas, M.V. Basin, Predictive output feedback control for networked control systems, *IEEE Trans. Ind. Electron.* 61 (January (1)) (2014) 512–519.
- [9] S. Hu, D. Yue, Event-based  $\mathcal{H}_\infty$  filtering for networked system with communication delay, *Signal Process.* 92 (2012) 2029–2039.
- [10] H. Wang, P. Shi, J. Zhang, Event-triggered fuzzy filtering for a class of nonlinear networked control systems, *Signal Process.* 113 (2015) 159–168.
- [11] M. Souza, G.S. Deaecto, J.C. Geromel, J. Daafouz, Self-triggered linear quadratic networked control, *Optim. Control Appl. Methods* 35 (5) (2014) 524–538.
- [12] M. Souza, J.C. Geromel,  $\mathcal{H}_2$  self-triggered dynamic output feedback for networked control, in: *52nd IEEE Annual Conference on Decision and Control*, Florence, Italy, 2013, pp. 4736–4741.
- [13] X. Wang, M.D. Lemmon, Self-triggered feedback control systems with finite-gain  $\mathcal{L}_2$  stability, *IEEE Trans. Autom. Control* 54 (March) (2009) 452–467.
- [14] X. Wang, M.D. Lemmon, Self-triggering under state-independent disturbances, *IEEE Trans. Autom. Control* 55 (June) (2010) 1494–1500.
- [15] E. Henriksson, D.E. Quevedo, H. Sandberg, K.H. Johansson, Self-triggered model predictive control for network scheduling and control, in: *8th IFAC Symposium on Advanced Control of Chemical Processes*, Singapore, 2012.
- [16] T.M.P. Gommans, D. Antunes, M.C.F. Donkers, P. Tabuada, W.P.M. H. Heemels, Self-triggered linear quadratic control, *Automatica* 50 (4) (2014) 1279–1287.
- [17] IEEE 802.15.4 standard: Wireless Medium Access Control (MAC) and Physical layer (PHY) specifications for low-rate Wireless Personal Area Networks (WPANs), IEEE 802.15.4, 2006, Available Online at: (<https://standards.ieee.org/getieee802/download/802.15.4-2011.pdf>).
- [18] A. Willig, Recent and emerging topics in wireless industrial communication, *IEEE Trans. Ind. Inf.* 4 (May) (2008) 102–124.
- [19] U. Tiberi, C. Fischione, K.H. Johansson, M.D. Di Benedetto, Energy-efficient sampling of networked control systems over IEEE 802.15.4 wireless networks, *Automatica* 49 (2013) 712–724.
- [20] P. Park, J. Araújo, K.H. Johansson, Wireless networked control system co-design, in: *Proceedings of the 2011 IEEE International Conference on Networking, Sensing and Control (ICNSC)*, Delft, the Netherlands, 2011, pp. 486–491.
- [21] P. Park, P.D. Marco, C. Fischione, K.H. Johansson, Delay distribution analysis of wireless personal area networks, in: *Proceedings of the IEEE Conference on Decision and Control*, Maui, HI, 2012, pp. 5864–5869.
- [22] P. Park, P.D. Marco, C. Fischione, K.H. Johansson, Modeling and optimization of the IEEE 802.15.4 protocol for reliable and timely communications, *IEEE Trans. Parallel Distrib. Syst.* 24 (March) (2013) 550–564.
- [23] P. Park, C. Fischione, K.H. Johansson, Modeling and stability analysis of hybrid multiple access in the IEEE 802.15.4 protocol, *ACM Trans. Sens. Netw.* 9 (2) .
- [24] U. Tiberi, C. Fischione, K.H. Johansson, M.D. Di Benedetto, Adaptive self-triggered control over IEEE 802.15.4 networks, in: *Proceedings of the 49th IEEE Conference on Decision and Control*, Atlanta, GA, 2010, pp. 2099–2104.
- [25] S. Xie, K.S. Low, E. Gunawan, An adaptive tuning algorithm for IEEE 802.15.4-based network control system, in: *Proceedings of the IEEE 9th International Conference on Intelligent Sensors, Sensor Networks and Information Processing (ISSNIP)*, Singapore, 2014, pp. 1–6.
- [26] M. Mazo Jr., P. Tabuada, On event-triggered and self-triggered control over sensor/actuator networks, in: *Proceedings of the 47th IEEE Conference on Decision and Control*, Cancun, Mexico, 2008, pp. 435–440.
- [27] J. Araújo, et al., Self-triggered control over wireless sensor and actuator networks, in: *International Conference on Distributed Computing in Sensor Systems and Workshops (DCOSS)*, 2011, pp. 1–9.
- [28] J. Araújo, et al., Self-triggered control for industrial wireless sensor and actuator networks, in: *Workshop on Real-Time Wireless for Industrial Applications at CPSWEEK*, Chicago, IL, 2011.
- [29] J. Araújo, et al., System architectures, protocol and algorithms for aperiodic wireless control systems, *IEEE Trans. Ind. Inf.* 10 (February) (2014) 175–184.